Importance of plasma injection events for energization of relativistic electrons in the Jovian magnetosphere

X. Tao,[1] R. M. Thorne,[1] R. B. Horne,[2] B. Ni,[1] J. D. Menietti,[3] Y. Y. Shprits,[1,4] and D. A. Gurnett[3]

[1]   Effects of density decrease in plasma injection regions and a latitude-dependent wave normal angle distribution on the energization of electrons by whistler mode waves at Jupiter are investigated. Previous work showed that whistler mode waves could enhance the fluxes of a few MeV electrons by an order of magnitude on a time scale of 30 days. However, density decrease in plasma injection regions and latitude dependence of the wave normal angle distribution of waves were not considered. Because this information is difficult to obtain from available observations, we perform a sensitivity study to demonstrate that the effect of density decrease on energization of electrons becomes important when the density inside injection regions is reduced to 25% of that outside. We also investigate the effect of a latitude-dependent wave normal angle distribution on energization of electrons using a ray tracing program and demonstrate that a realistic latitude-dependent wave normal angle distribution increases the rate of pitch angle diffusion near the loss cone, and thus enhances the loss rate, of 1–3 MeV electrons. However, the flux of 10 MeV electrons is not significantly affected. Results of the work are useful for understanding energization of MeV electrons at Jupiter, especially when combined with observations from future missions.

Citation: Tao, X., R. M. Thorne, R. B. Horne, B. Ni, J. D. Menietti, Y. Y. Shprits, and D. A. Gurnett (2011), Importance of plasma injection events for energization of relativistic electrons in the Jovian magnetosphere, *J. Geophys. Res.*, *116*, A01206, doi:10.1029/2010JA016108.

1.   Introduction

[2]   Resonant interactions between electrons and whistler mode waves play a controlling role on terrestrial radiation belt dynamics [*Kennel and Petschek*, 1966; *Lyons and Thorne*, 1973; *Summers et al.*, 1998; *Horne and Thorne*, 1998; *Horne et al.*, 2005b]. The resonant interactions occur when the Doppler-shifted wave frequency felt by an electron is equal to a multiple of electron's cyclotron frequency [e.g., *Stix*, 1992]. These interactions have been shown to be responsible for the energization of relativistic electrons in the outer radiation belt after a geomagnetic storm [*Horne et al.*, 2005b; *Shprits et al.*, 2006], and the refilling of the electron slot between the inner and outer radiation belts [*Thorne et al.*, 2007].

[3]   Strong whistler mode waves have also been observed at Jupiter [*Gurnett et al.*, 1996; *Thorne et al.*, 1997; *Bolton et al.*, 1997; *Xiao et al.*, 2003]. Recently, *Horne et al.* [2008] demonstrated that interactions between electrons and whistler mode waves in the Jovian magnetosphere cause significant acceleration of MeV electrons on a time scale of 30 days. Using wave power spectral density from Galileo measurements, *Horne et al.* [2008] calculated quasi-linear pitch angle and energy diffusion coefficients and solved a two dimensional diffusion equation at 10 R_J. They showed that fluxes of 1–6 MeV electrons increased by more than an order of magnitude within 30 days.

[4]   In the calculation of *Horne et al.* [2008], an empirical electron density model was used in calculation of diffusion coefficients. The empirical electron density model, however, does not consider the observed density decrease within plasma injection regions. Jupiter's magnetosphere, similar to Saturn's magnetosphere, is dominated by the centrifugal force because of its rapid rotation. Inward transport of hot and tenuous plasma and outward transport of cold and dense plasma has been proposed theoretically as a result of the centrifugal force dominated convection and an internal plasma source [*Hill*, 1976; *Hill et al.*, 1981]. Inside local plasma injection regions, electron density is typically smaller than the average ambient density by more than a factor of two, as argued by *Thorne et al.* [1997] and *Kivelson et al.* [1997]. Similar density cavities have been observed by Cassini at Saturn [e.g., *Menietti et al.*, 2008b; *Rymer et al.*, 2009]. A

[1]Department of Atmospheric and Oceanic Sciences, University of California, Los Angeles, California, USA.
[2]British Antarctic Survey, Cambridge, UK.
[3]Department of Physics and Astronomy, University of Iowa, Iowa City, Iowa, USA.
[4]Institute of Geophysics and Planetary Physics, University of California, Los Angeles, California, USA.
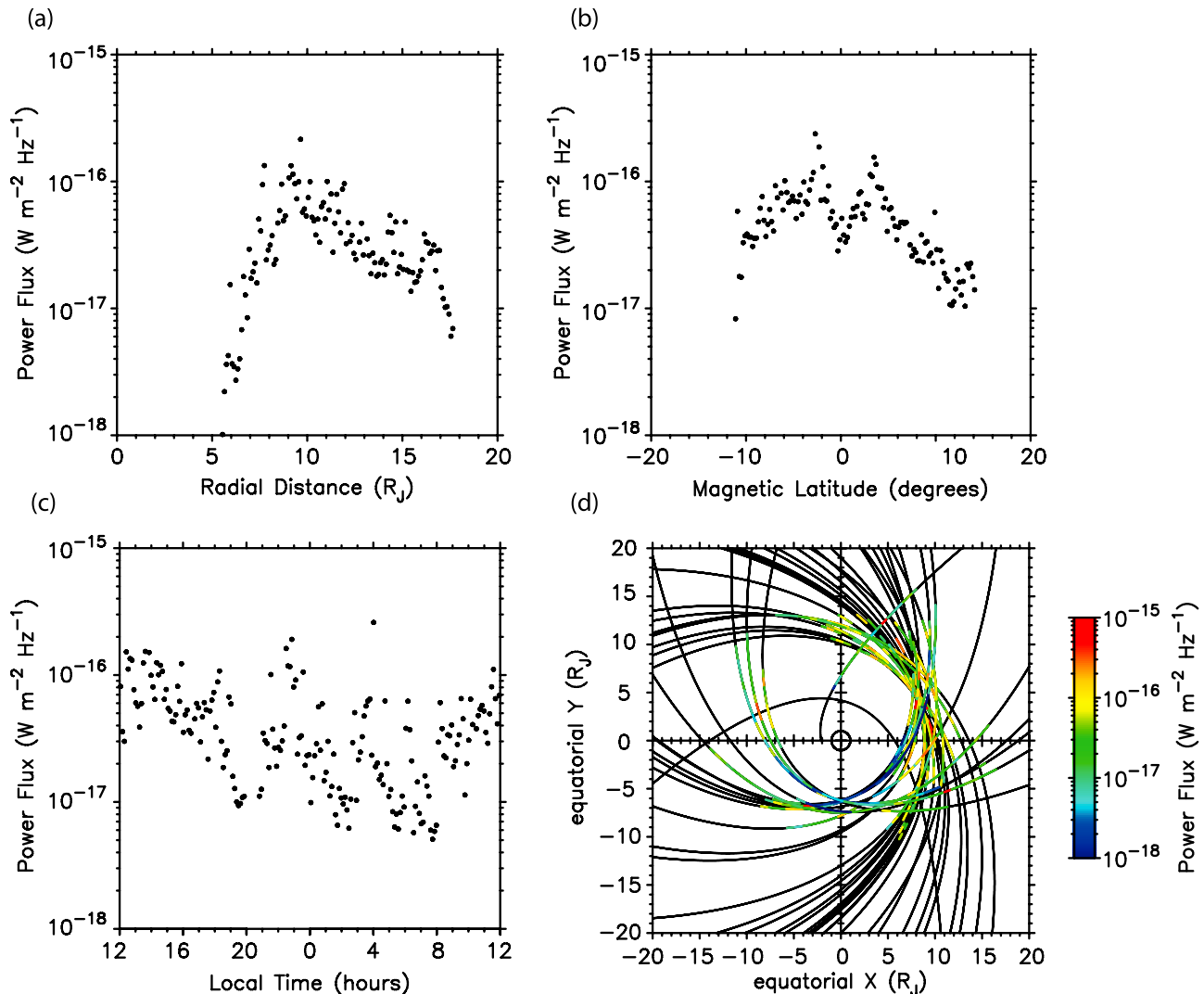
Figure 1. Average whistler mode wave intensities measured by Galileo as a function of (a) radial distance, (b) magnetic latitude, and (c) local time. (d) The Galileo orbits are plotted together with color-coded whistler mode wave intensities (power flux).

decrease in electron density has been shown to favor local stochastic energization [*Horne et al.*, 2003]. Consequently taking the density decrease inside injection regions into consideration would be important to quantify the energization time scale.

[5] The wave normal angle distribution of chorus wave power is another important factor that is hard to determine from observation, but is required in the calculation of the diffusion coefficients. *Horne et al.* [2008] assumed that the wave power peaks around wave normal angle $\psi = 0°$, based on previous studies on terrestrial whistler mode chorus waves [*Horne et al.*, 2005a; *Li et al.*, 2007]. However, several ray tracing studies and observations have shown that whistler waves tend to become more oblique at higher latitudes even when starting parallel from the equator [*Bortnik et al.*, 2008; *Li et al.*, 2008, 2009; *Haque et al.*, 2010]. Since the wave power might not always peak around $\psi = 0°$, we

will analyze the effect of a different wave normal angle distribution of whistler wave power on our results.

[6] In this work, we follow the modeling of *Horne et al.* [2008], but also take into consideration cross diffusion terms $D_{\alpha p}$, which have been shown to be important for quantifying wave particle interactions in the terrestrial magnetosphere [*Albert and Young*, 2005; *Tao et al.*, 2008, 2009; *Xiao et al.*, 2009]. The sensitivity of the main conclusions of *Horne et al.* [2008] to the amount of density decrease inside the local plasma injection regions is analyzed in section 3.2. A ray tracing code HOTRAY [*Horne*, 1989] is then used to trace several whistler wave rays from the equator to higher latitudes to investigate change of their wave normal angle. The results are used to construct a latitude-dependent wave normal angle distribution model, which is then used to calculate quasi-linear diffusion coefficients. The effect of the latitude-dependent wave normal
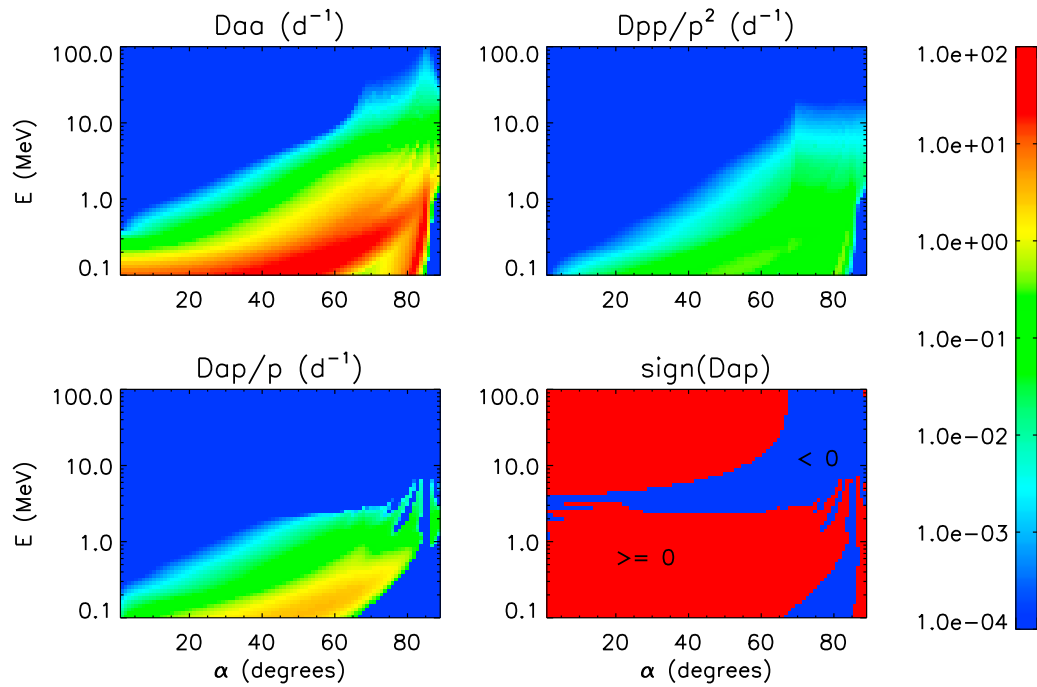
Figure 2. Bounce-averaged diffusion rates (d^{-1}) obtained using a density model outside injection regions assuming that the wave normal angle distribution is centered around $0°$. (bottom right) The sign of $D_{\alpha p}$.
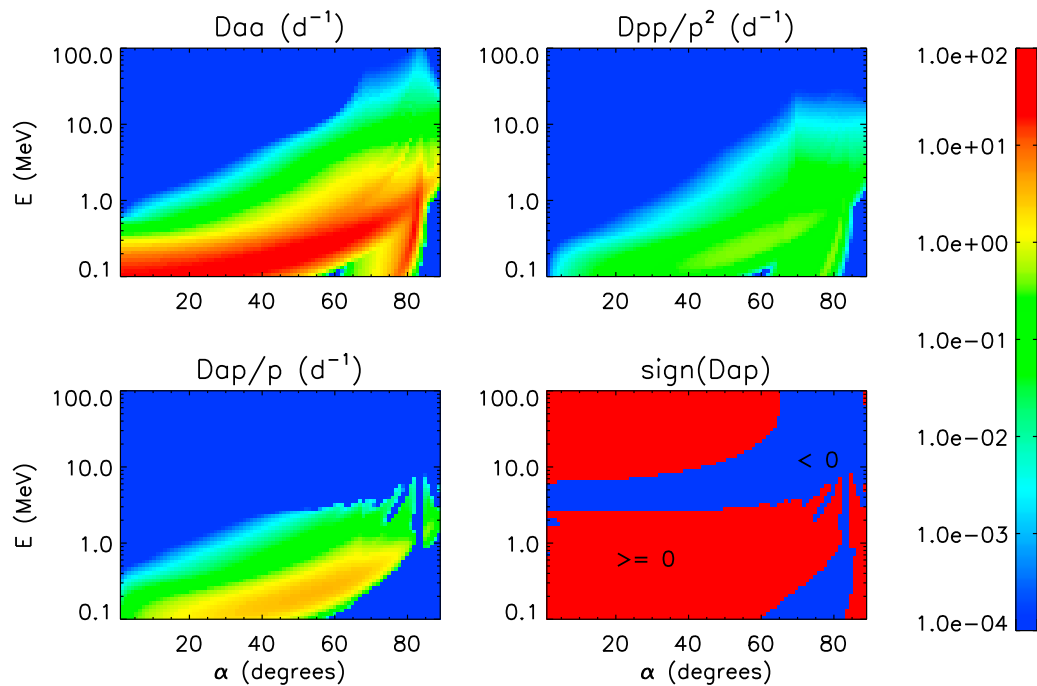

Figure 3. Same as Figure 2 but for D_{hd} (the plasma density is assumed to be half of that used in calculating D_o).
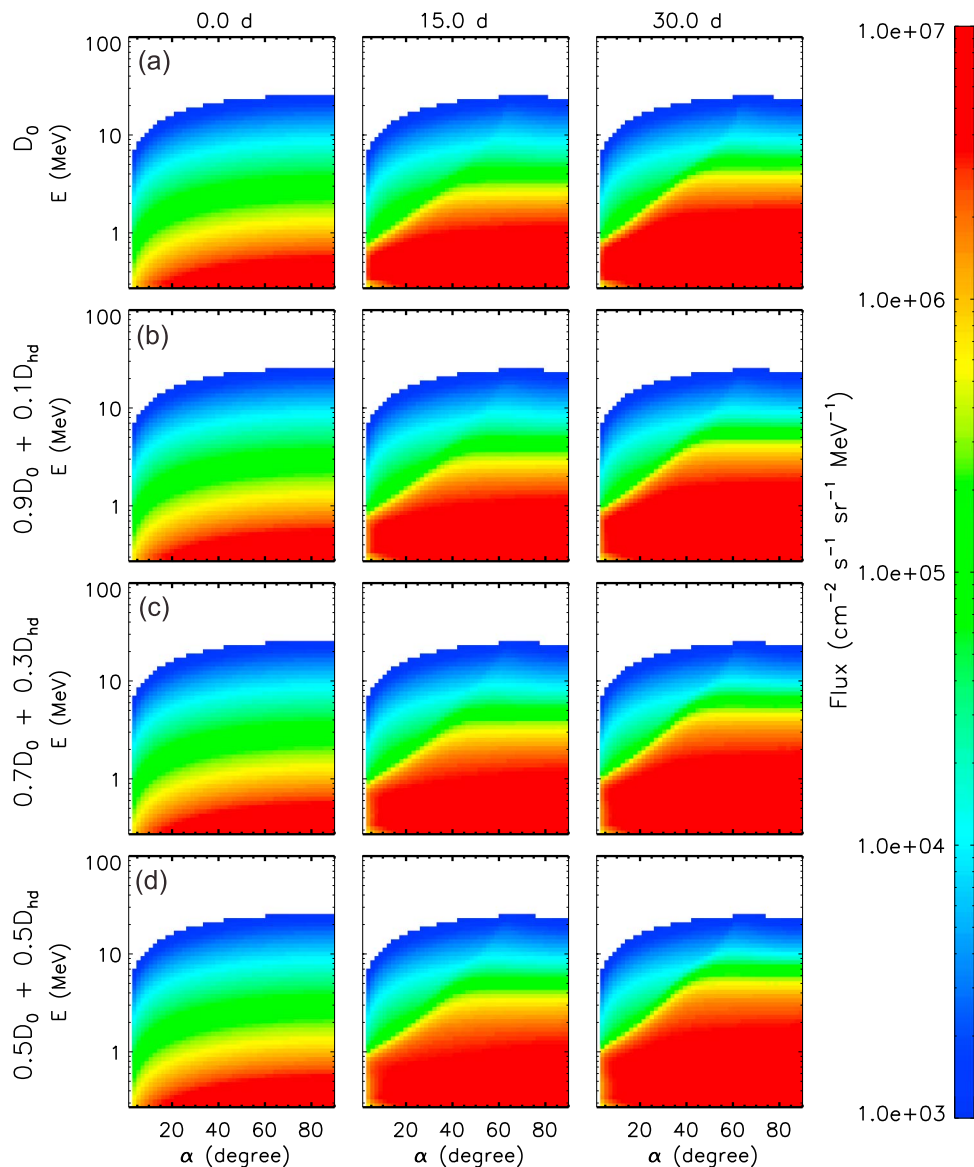
Figure 4. Electron fluxes (color coded) at (left) 0 days, (middle) 15 days, and (right) 30 days as a function of α and E for (a) D_o, (b) $0.9D_o + 0.1D_{hd}$, (c) $0.7D_o + 0.3D_{hd}$, and (d) $0.5D_o + 0.5D_{hd}$.

angle distribution on electron flux evolution is described in section 3.3. Finally, we summarize our work in section 4.

2. Observed Wave Power Distribution and Quasi-Linear Diffusion Coefficients

[7] We use a survey of all wave data recorded by the Galileo Plasma Wave Subsystem (PWS) instrument [*Gurnett et al.*, 1992] from 27 June 1996 to 5 November 2002. The wave power distribution of whistler mode waves in Jupiter's inner magnetosphere is shown in Figure 1, as a function of magnetic latitude or local time at 10 R_J, or radial distance. Also shown in Figure 1d is the wave power flux plotted together with Galileo orbits. It is seen from Figure 1 that strong waves are detected between 6 R_J and 18 R_J, peaking between 8 R_J and 10 R_J. The whistler wave power peaks between 2° and 4° in latitude, and decreases by an order of

magnitude at the highest latitude (~12°) sampled by Galileo. The wave power flux distribution also shows a day-night asymmetry and is slightly stronger in the dayside near local noon. A more detailed analysis of whistler mode chorus waves observed by Galileo could be found in work by *Menietti et al.* [2008a].

[8] As argued by *Horne et al.* [2008], the preferred location for strong electron energization is outside the Io torus, where the electron density is low and wave activity is strong. The ratio of electron plasma frequency to cyclotron frequency ω_{pe}/ω_{ce} is about 5 at 10 R_J. Also due to the strong centrifugal force, plasma is confined to the centrifugal equator, thus ω_{pe}/ω_{ce} falls to a relatively low value at higher latitudes. We follow *Horne et al.* [2008] and use a plasma density model by *Bagenal* [1994] for the electron density distribution along a magnetic field line outside injection events at Jupiter. Because there are insufficient measure-
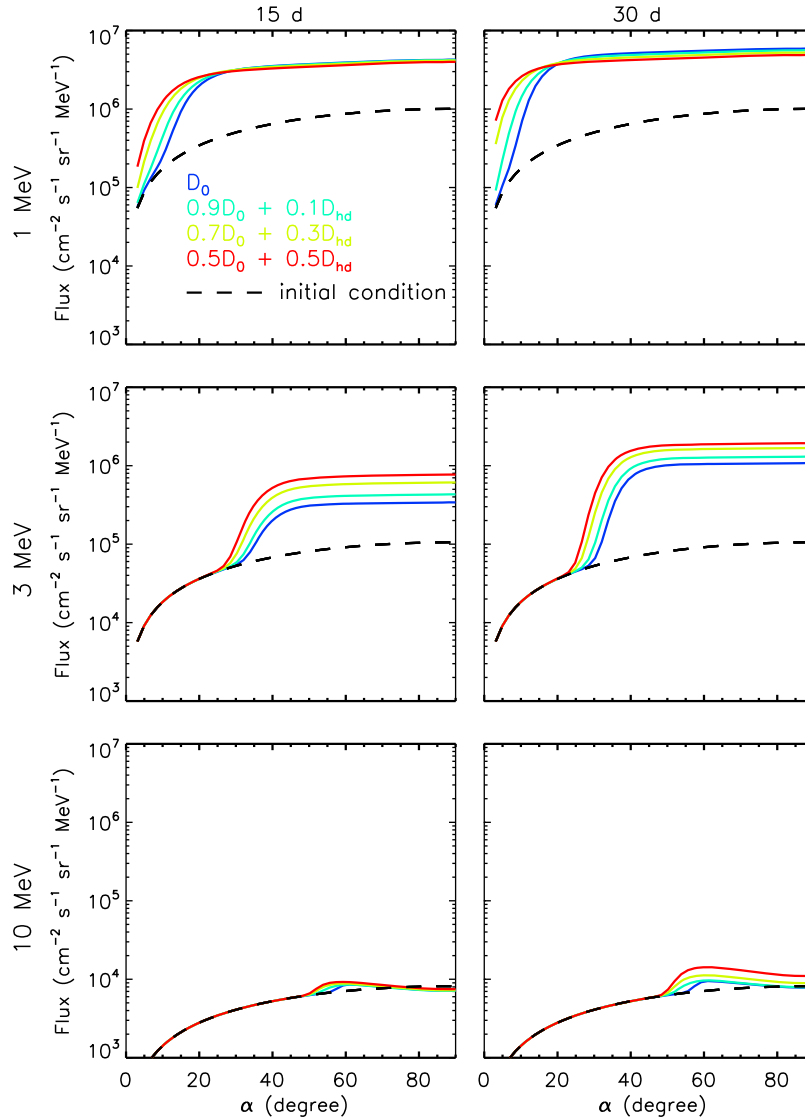
Figure 5. Line plots of electron fluxes of (top) 1 MeV, (middle) 3 MeV, and (bottom) 10 MeV at (left) 15 days and (right) 30 days due to different combinations of D_o and D_{hd} indicated by different colors. Initial conditions are shown by dashed lines.

ments of electron density inside plasma injection regions, we will assume the electron density inside injection regions to be either half or one quarter of the electron density outside injection events to test the sensitivity of our results to the density decrease in injection regions.

[9] To calculate quasi-linear diffusion coefficients, we assume the wave power to be Gaussian in frequency [*Glauert and Horne*, 2005]. *Horne et al.* [2008] showed that chorus is strongest near $0.1 \sim 0.2\omega_{ce}$. We follow *Horne et al.* [2008] and assume that the wave power peaks at $0.15\omega_{ce}$ with a width of $0.05\omega_{ce}$. The wave normal angle distribution in $X \equiv \tan \psi$ is assumed to be Gaussian, similar to chorus waves at Earth, with a width $X_w = \tan 30°$. The wave power is first assumed to be centered at $X_c = 0°$, but we also investigate effects of a latitude-dependent wave normal angle distribution on electron energization in section 3.3. Using the Full Diffusion Code [*Shprits and Ni*, 2009; *Ni*

et al., 2008], we first calculate the diffusion coefficients outside injection events (hereafter denoted as D_o) as shown in Figure 2.

3. Evolution of Electron Phase Space Densities

3.1. Description of the Numerical Model

[10] A 2-D bounce-averaged diffusion equation is used to model the evolution of electron phase space density (f) as a function of equatorial pitch angle (α) and momentum (p):

$$\frac{\partial f}{\partial t} = \frac{1}{Gp} \frac{\partial}{\partial \alpha} G \left(D_{\alpha\alpha} \frac{1}{p} \frac{\partial f}{\partial \alpha} + D_{\alpha p} \frac{\partial f}{\partial p} \right)$$
$$+ \frac{1}{G} \frac{\partial}{\partial p} G \left(D_{\alpha p} \frac{1}{p} \frac{\partial f}{\partial \alpha} + D_{pp} \frac{\partial f}{\partial p} \right), \quad (1)$$
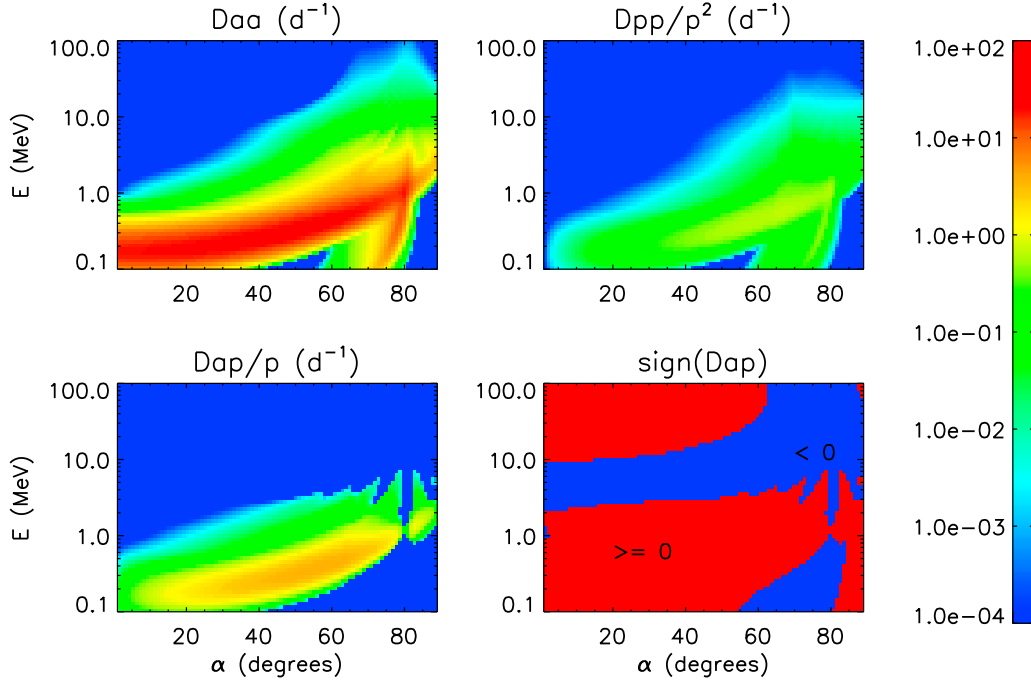
Figure 6. Same as Figure 2 but for D_{qd} (the plasma density is assumed to be a quarter of that used in calculating D_o).

where $D_{\alpha\alpha}$, $D_{\alpha p}$ and D_{pp} are bounce-averaged pitch angle, mixed and momentum diffusion coefficients. Here G is a Jacobian factor, $G = p^2 T(\alpha) \sin(\alpha) \cos(\alpha)$, and $T(\alpha) \approx 1.30 - 0.56 \sin(\alpha)$ is the normalized bounce period. In work by *Horne et al.* [2008], the equation is solved without mixed terms $D_{\alpha p}$. However, the importance of $D_{\alpha p}$ has been shown by previous work and several methods have also been proposed to solve equation (1) [*Albert and Young*, 2005; *Tao et al.*, 2008, 2009; *Xiao et al.*, 2009]. In this work, we use the numerical method of *Albert and Young* [2005] to solve equation (1) with $D_{\alpha p}$ included.

[11] The initial and boundary conditions are chosen to be the same as those of *Horne et al.* [2008]. To minimize effects of wave particle interactions in the initial distribution at 10 R_J, the average electron flux from Pioneer and Voyager data at 15.75 R_J is used to calculate the initial electron flux at 10 R_J, assuming a dipole magnetic field and loss-free inward radial diffusion to 10 R_J. The electron flux is then converted to phase space density using $f = j/p^2$. We fix phase space density at the lower energy boundary at $E = 300$ keV and set $f = 0$ at $E = 100$ MeV. We also assume that electrons scattered into the loss cone ($\alpha_{LC} = 1.5°$) precipitate into the Jovian atmosphere within a quarter of the bounce time. At $\alpha = 90°$, we assume $\partial f/\partial \alpha = 0$.

3.2. Sensitivity to Density Decrease During Local Plasma Injection Regions

[12] Within plasma injection regions, the total plasma density is decreased by at least a factor of two, as inferred from enhancement of magnetic field inside the injection region and the requirement of the total pressure balance [*Thorne et al.*, 1997; *Kivelson et al.*, 1997]. A decrease in

total electron density will affect both the resonance energy of electrons and the pitch angle and energy diffusion coefficients. A smaller electron density will result in larger wave phase speed and correspondingly will enhance energy diffusion. Thus including density decrease in the modeling may be important to calculate the time scale of electron energization.

[13] However, as far as we are aware, there is no density model for plasma injection regions and no direct measurement of the fraction (χ_i) of plasma injection regions in terms of local time. To investigate the effects of local plasma injections on the average rate of energization of electrons by whistler mode waves, we assume different values for χ_i and average densities ρ_i of plasma injection regions. The drift-averaged diffusion coefficient used in equation (1) is $\mathbf{D} = \chi_i \mathbf{D}_i + (1 - \chi_i)\mathbf{D}_o$, where $\mathbf{D}_i$ is the diffusion coefficient inside an injection region.

3.2.1. Case 1: $\rho_i = (1/2)\rho_o$

[14] We calculate the diffusion coefficients using the wave model described in section 2 but with the electron density ρ_i half of that outside (ρ_o) and three values for χ_i. The resulting diffusion coefficient $\mathbf{D}_i = \mathbf{D}_{hd}$ is shown in Figure 3. The evolution of electron fluxes is shown in Figure 4 with Figure 4a showing the results of using the diffusion coefficient $\mathbf{D}_o$ discussed in section 2, and Figures 4b–4d exhibiting changes due to the increasing probability of observing an injection event. Corresponding line plots of fluxes of 1 MeV, 3 MeV, and 10 MeV electrons are shown in Figure 5, which indicated that increasing χ_i will increase fluxes at 3 MeV and 10 MeV electrons, mainly because of the increase of energy diffusion. However, fluxes at 1 MeV at larger pitch angles are slightly reduced because of the
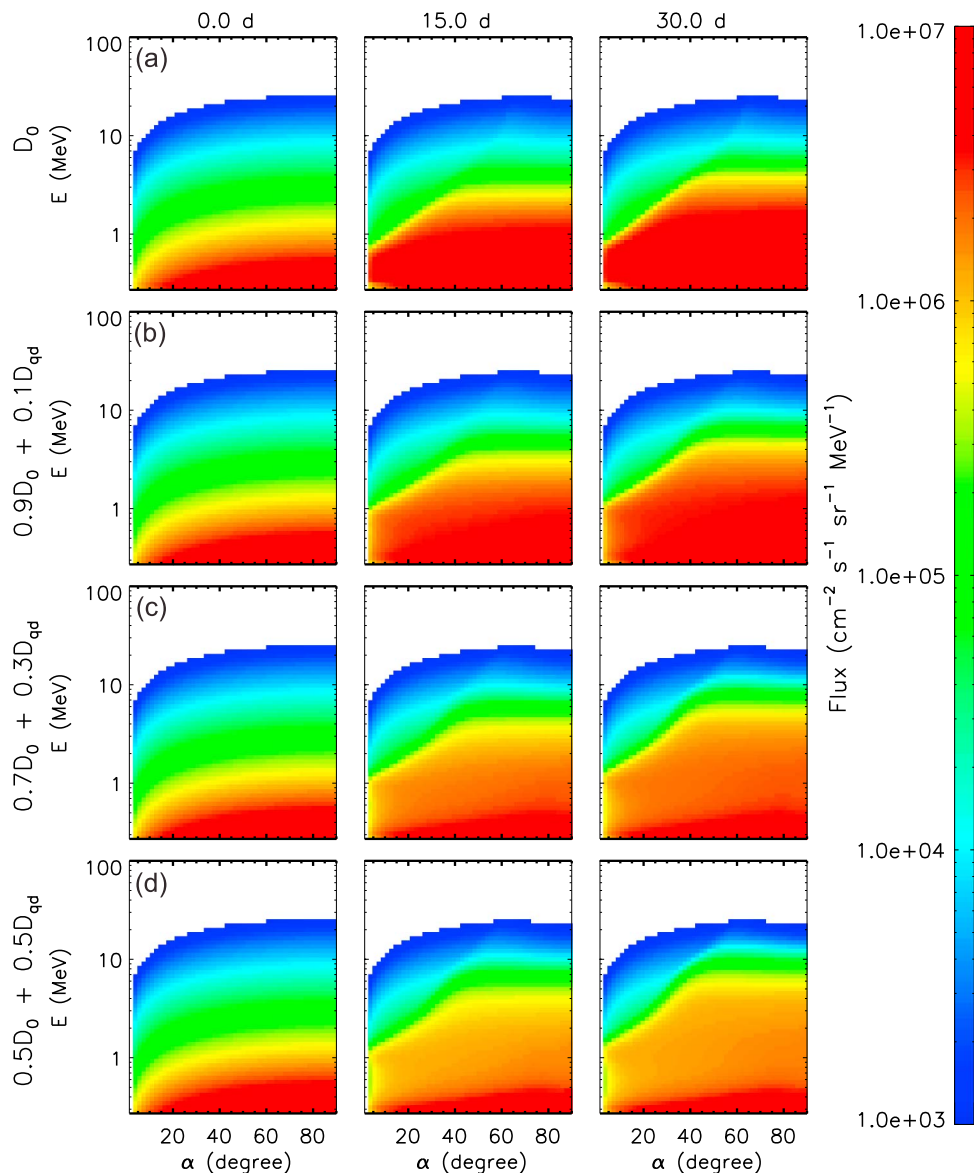
Figure 7. Same as Figure 4 but due to combinations of D_o and D_{qd}.

increased pitch angle diffusion near loss cone. Overall, when $\rho_i = (1/2)\rho_o$, including density decrease inside injection regions will slightly decrease fluxes of 1 MeV electrons at higher pitch angles and increase fluxes at 3 MeV and 10 MeV electrons by a factor of 1.5. Consequently the density decrease inside injection regions in the case of $\rho_i = (1/2)\rho_o$ does not seem to significantly affect the time scale of energization.

3.2.2. Case 2: $\rho_i = (1/4)\rho_o$

[15] For the case of $\rho_i = (1/4)\rho_o$, the diffusion coefficient $D_i = D_{qd}$ is presented in Figure 6, which shows both higher energy and pitch angle diffusion coefficients at higher energies ($E > 1$ MeV), compared with Figure 2. The evolution of 2-D electron fluxes due to different χ_i with D_{qd} is shown in Figure 7, and the line plots of fluxes at 1 MeV, 3 MeV and 10 MeV are shown in Figure 8. Significant effects of including D_{qd} occur even when $\chi_i = 0.1$, where

the electron flux at 10 MeV is increased due to increased energy diffusion, while that at 1 MeV is decreased due to increased pitch angle diffusion near the loss cone. When i_i is increased to 0.5, the electron flux at 10 MeV around 55° is increased by a factor of 5 at t = 30 days, and the electron flux at 1 MeV is decreased by a factor of 3 for pitch angles larger than about 20°. Overall, a density decrease by a factor of 4 inside injection regions would appear to have an important effect on the time scale of electron energization.

3.3. Effects of a Latitude-Dependent Wave Normal Angle Distribution

[16] The wave normal distribution of chorus waves was assumed to be centered around 0° [e.g., *Horne et al.*, 2008] in the above wave model used to calculate D_o. However, several ray tracing studies [*Bortnik et al.*, 2008; *Li et al.*,
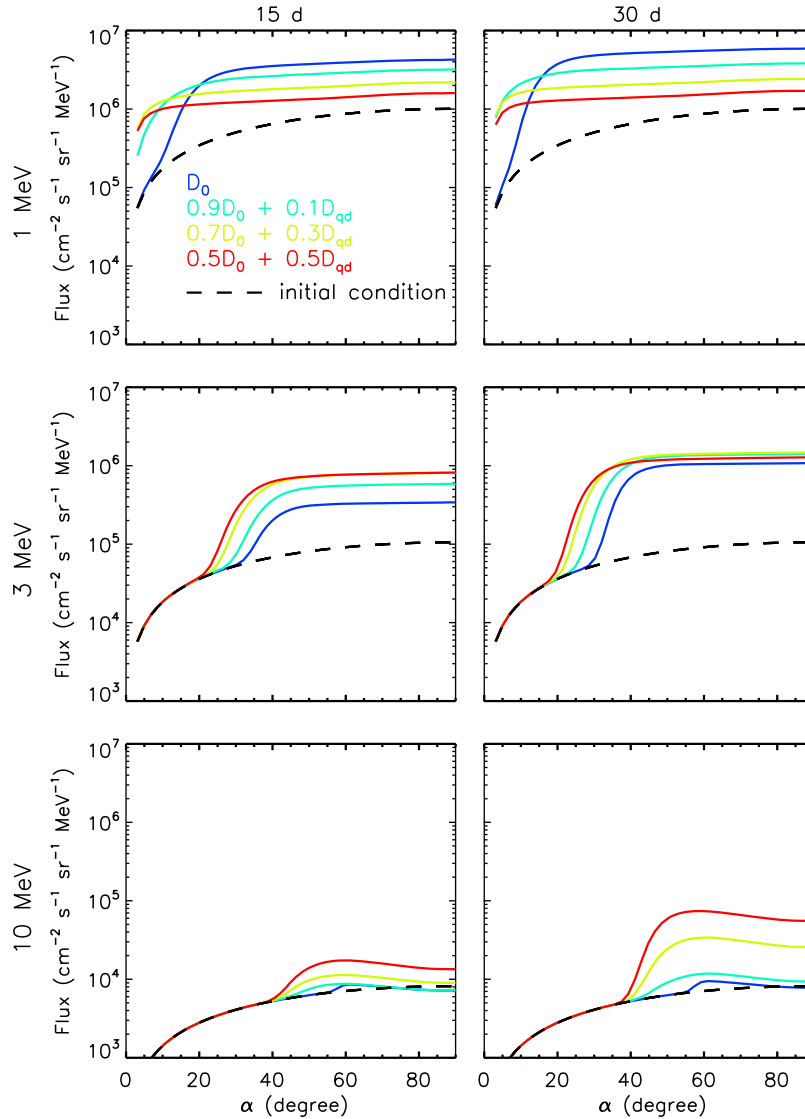
Figure 8. Same as Figure 5 but due to combinations of D_o and D_{qd}.

2008] have shown that the wave normal angle of an initially parallel propagating ray normally increases during its propagation away from the equator. Here, we use a ray tracing code HOTRAY [*Horne*, 1989] to show the propagation of whistler mode waves in the Jovian magnetosphere and subsequently take the effects of the latitude-dependent wave normal angle distribution into account in the calculation of quasi-linear diffusion coefficients.

[17] The HOTRAY code was developed by *Horne* [1989] to trace electromagnetic and electrostatic waves in a hot magnetized plasma. We use HOTRAY code to trace rays of whistler mode chorus waves of several frequencies, starting with $\psi = 0°$ from the equatorial plane at $L = 10$. The resulting variation of the wave normal angle with respect to latitude λ is shown in Figure 9, which shows that from $\lambda = 0°$ to $10°$, the wave normal angles of all rays ($f = 0.05f_{ce}$ to $0.25f_{ce}$) change from $0°$ to about $40°$. Consequently, we use a latitude-dependent wave normal distribution in the cal-

culation of diffusion coefficients based on the ray tracing result ($\psi_c = -0.36 + 5.04\lambda - 0.06\lambda^2$ and $X_c = \tan(\psi_c)$). Other parameters of the wave model are the same as the one described in section 2. The resulting diffusion coefficient $D_{\psi_c(\lambda)}$ is shown in Figure 10. The evolution of electron fluxes calculated using $D_{\psi_c(\lambda)}$ at 1 MeV, 3 MeV, and 10 MeV is shown in Figure 11, compared with that due to D_o. The fluxes of 10 MeV electrons calculated using $D_{\psi_c(\lambda)}$ and D_o are almost the same. However, the pitch angle diffusion at lower pitch angles near the loss cone is increased when using $D_{\psi_c(\lambda)}$, resulting in more losses of 1 MeV and 3 MeV electrons and a decrease in their fluxes.

4. Discussion and Summary

[18] We used a wave power distribution obtained from a survey of Galileo PWS wave records between 27 June 1996 and 5 November 2002 to investigate the effects of density
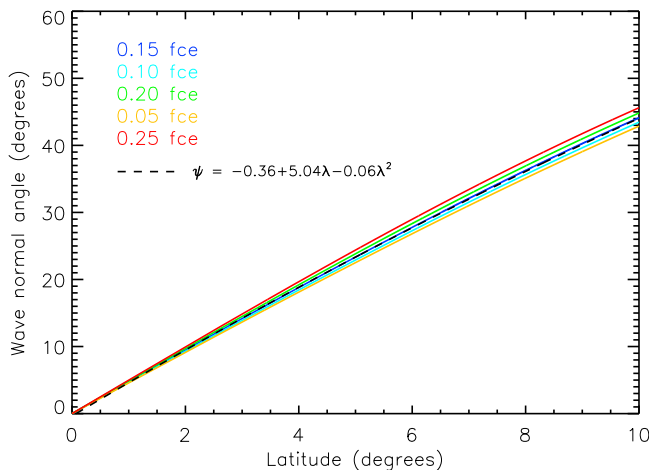
Figure 9. Evolution of the wave normal angle (ψ) of rays at different frequencies, indicated by different colors, as a function of latitude. The black dashed line is $\psi = -0.36 + 5.04\lambda - 0.06\lambda^2$.

decrease in injection regions and a latitude-dependent wave normal angle distribution of whistler mode waves on energization of electrons. We assumed two different average densities (ρ_i) of the injection regions and we demonstrated that if ρ_i is half of the density outside (ρ_o), the effects of density decrease on the time scale of electron energization are negligible. However, if ρ_i is a quarter of ρ_o, the effect of density decrease on the time scale of energization of higher-energy (10 MeV) electrons is important when the fraction (χ_i) of plasma injection regions in local time is larger than

0.3. Also, including the injection regions will also enhance pitch angle diffusion of lower energy (1 MeV and 3 MeV) electrons near loss cone, thus reducing their fluxes. One thing that is missing from our model is the enhancement of whistler mode wave activity during plasma injection regions, which will be left to future work.

[19] The effect of a latitude-dependent wave normal angle distribution of whistler waves on evolution of electron phase space density was also investigated with the aid of a ray tracing code HOTRAY. We showed that rays of whistler waves initially parallel to local magnetic field have a wave normal angle of about 40° when reaching 10° in latitude. The latitude-dependent wave normal angle distribution has no obvious effect on 10 MeV electron fluxes. However, it increases pitch angle diffusion of 1 MeV and 3 MeV electrons near the loss cone and reduces their fluxes by about a factor of 3. Thus the change of wave normal angle of chorus waves during propagation should be taken into account when quantitatively modeling electron flux evolution of Jovian electrons.

[20] Other parameters that are potentially important but not discussed in this study are, e.g., initial conditions [*Xiao et al.*, 2010], the width of the frequency and wave normal angle distributions. We used initial conditions calculated from observations, but it might also be possible to use kappa-type distributions [*Xiao et al.*, 2008], which have been shown to fit very well with observed electron distributions at Earth. Investigating the importance of these parameters are left to future work. Overall, better information of these parameters might be provided by future missions to Jupiter, and the results of this work should be useful to understand relativistic electron dynamics at Jupiter when combined with more observations.
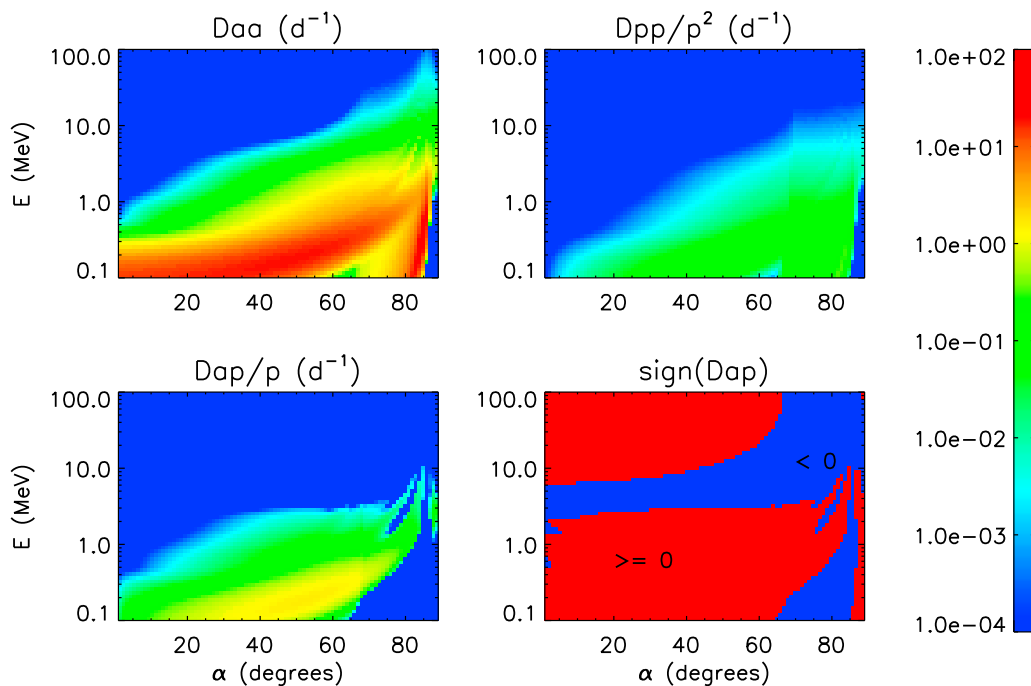

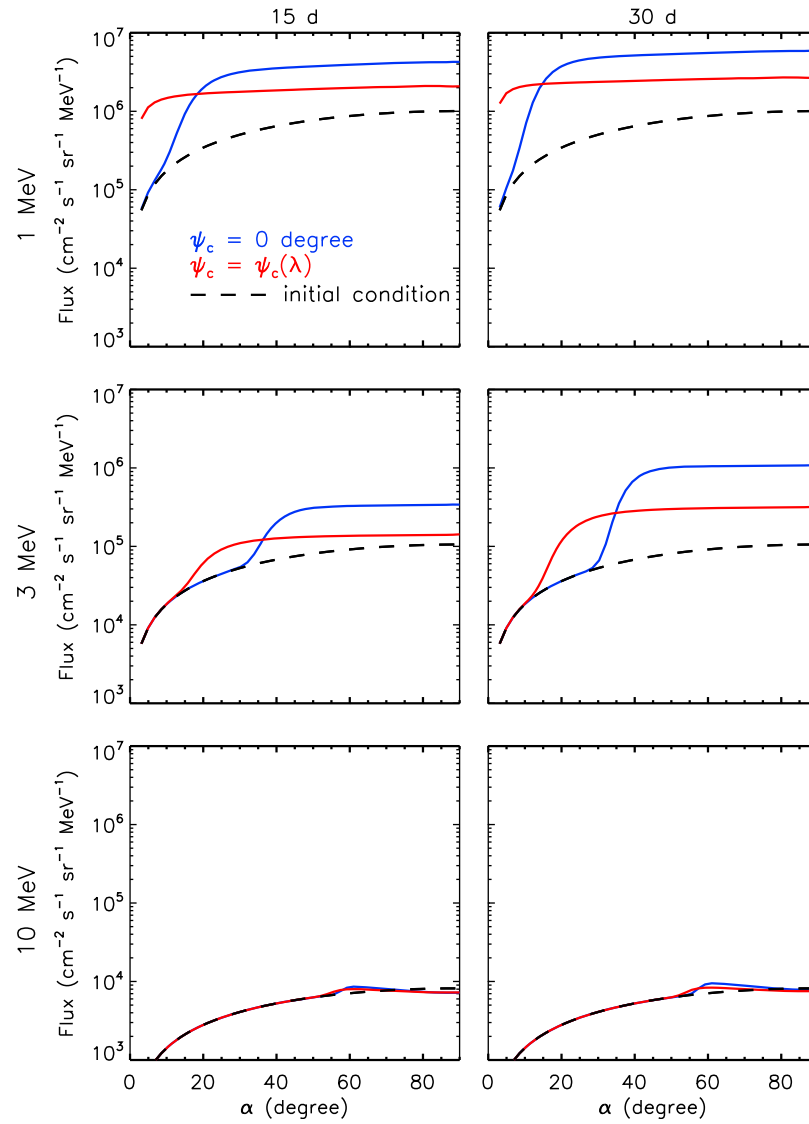**Figure 10.** Same as Figure 2 but for $\boldsymbol{D}_{\psi_c}(\lambda)$ (the wave normal angle distribution is latitude dependent).

Figure 11. Evolution of electron fluxes at 15 and 30 days using $\boldsymbol{D}_o$ (blue) and $\boldsymbol{D}_{\psi_c}(\lambda)$ (red) for (top) 1 MeV, (middle) 3 MeV, and (bottom) 10 MeV.

References

Albert, J. M., and S. L. Young (2005), Multidimensional quasi-linear diffusion of radiation belt electrons, *Geophys. Res. Lett.*, *32*, L14110, doi:10.1029/2005GL023191.

Bagenal, F. (1994), Empirical model of the Io plasma torus: Voyager measurements, *J. Geophys. Res.*, *99*(A6), 11,043–11,062.

Bolton, S. J., R. M. Thorne, D. A. Gurnett, W. S. Kurth, and D. J. Williams (1997), Enhanced whistler-mode emissions: Signatures of interchange motion in the Io torus, *Geophys. Res. Lett.*, *24*(17), 2123–2126.

Bortnik, J., R. M. Thorne, and N. P. Meredith (2008), The unexpected origin of plasmaspheric hiss from discrete chorus emissions, *Nature*, *452*, 62–66, doi:10.1038/nature06741.

Glauert, S. A., and R. B. Horne (2005), Calculation of pitch angle and energy diffusion coefficients with the PADIE code, *J. Geophys. Res.*, *110*, A04206, doi:10.1029/2004JA010851.

Gurnett, D. A., W. S. Kurth, R. R. Shaw, A. Roux, R. Gendrin, C. F. Kennel, F. L. Scarf, and S. D. Shawhan (1992), The Galileo plasma wave investigation, *Space Sci. Rev.*, *60*, 341–355, doi:10.1007/BF00216861.

Gurnett, D. A., W. S. Kurth, A. Roux, S. J. Bolton, and C. F. Kennel (1996), Galileo plasma wave observations in the Io plasma torus and near Io, *Science*, *274*, 391–392.

Haque, N., M. Spasojevic, O. Santolík, and U. S. Inan (2010), Wave normal angles of magnetospheric chorus emissions observed on the Polar spacecraft, *J. Geophys. Res.*, *115*, A00F07, doi:10.1029/2009JA014717.

Hill, T. W. (1976), Interchange stability of a rapidly rotating magnetosphere, *Planet. Space Sci.*, *24*, 1151–1154.

Hill, T. W., A. J. Dessler, and L. J. Maher (1981), Corotating magnetospheric convection, *J. Geophys. Res.*, *86*(A11), 9020–9028.

Horne, R. B. (1989), Path-integrated growth of electrostatic waves: The generation of terrestrial myriametric radiation, *J. Geophys. Res.*, *94*(A7), 8895–8909.

Horne, R. B., and R. M. Thorne (1998), Potential waves for relativistic electron scattering and stochastic acceleration during magnetic storms, *Geophys. Res. Lett.*, *25*(15), 3011–3014.

Horne, R. B., S. A. Glauert, and R. M. Thorne (2003), Resonant diffusion of radiation belt electrons by whistler-mode chorus, *Geophys. Res. Lett.*, *30*(9), 1493, doi:10.1029/2003GL016963.

Horne, R. B., R. M. Thorne, S. A. Glauert, J. M. Albert, N. P. Meredith, and R. R. Anderson (2005a), Timescale for radiation belt electron acceleration by whistler mode chorus waves, *J. Geophys. Res.*, *110*, A03225, doi:10.1029/2004JA010811.

Horne, R. B., et al. (2005b), Wave acceleration of electrons in the Van Allen radiation belts, *Nature*, *437*, 227–230, doi:10.1038/nature03939.

Horne, R. B., R. M. Thorne, S. A. Glauert, J. D. Menietti, Y. Y. Shprits, and D. A. Gurnett (2008), Gyro-resonant electron acceleration at Jupiter, *Nat. Phys.*, *4*, 301–304, doi:10.1038/nphys897.

Kennel, C. F., and H. E. Petschek (1966), Limit on stably trapped particle fluxes, *J. Geophys. Res.*, *71*(1), 1–28.

Kivelson, M. G., K. K. Khurana, C. T. Russell, and R. J. Walker (1997), Intermittent short-duration magnetic field anomalies in the Io torus: Evidence for plasma interchange?, *Geophys. Res. Lett.*, *24*(17), 2127–2130.

Li, W., Y. Y. Shprits, and R. M. Thorne (2007), Dynamic evolution of energetic outer zone electrons due to wave-particle interactions during storms, *J. Geophys. Res.*, *112*, A10220, doi:10.1029/2007JA012368.

Li, W., R. M. Thorne, N. P. Meredith, R. B. Horne, J. Bortnik, Y. Y. Shprits, and B. Ni (2008), Evaluation of whistler mode chorus amplification during an injection event observed on CRRES, *J. Geophys. Res.*, *113*, A09210, doi:10.1029/2008JA013129.

Li, W., et al. (2009), Evaluation of whistler-mode chorus intensification on the nightside during an injection event observed on the THEMIS spacecraft, *J. Geophys. Res.*, *114*, A00C14, doi:10.1029/2008JA013554.

Lyons, L. R., and R. M. Thorne (1973), Equilibrium structure of radiation belt electrons, *J. Geophys. Res.*, *78*(13), 2142–2149.

Menietti, J. D., R. B. Horne, D. A. Gurnett, G. B. Hospodarsky, C. W. Piker, and J. B. Groene (2008a), A survey of Galileo plasma wave instrument observations of Jovian whistler-mode chorus, *Ann. Geophys.*, *26*, 1819–1828.

Menietti, J. D., O. Santoík, A. M. Rymer, G. B. Hospodarsky, A. M. Persoon, D. A. Gurnett, A. J. Coates, and D. T. Young (2008b), Analysis of plasma waves observed within local plasma injections seen in Saturn's magnetosphere, *J. Geophys. Res.*, *113*, A05213, doi:10.1029/2007JA012856.

Ni, B., R. M. Thorne, Y. Y. Shprits, and J. Bortnik (2008), Resonant scattering of plasma sheet electrons by whistler-mode chorus: Contribution to diffuse auroral precipitation, *Geophys. Res. Lett.*, *35*, L11106, doi:10.1029/2008GL034032.

Rymer, A., et al. (2009), Cassini evidence for rapid interchange transport at Saturn, *Planet. Space Sci.*, *57*, 1779–1784, doi:10.1016/j.pss.2009.04.010.

Shprits, Y. Y., and B. Ni (2009), Dependence of the quasi-linear scattering rates on the wave normal distribution of chorus waves, *J. Geophys. Res.*, *114*, A11205, doi:10.1029/2009JA014223.

Shprits, Y. Y., R. M. Thorne, R. B. Horne, S. A. Glauert, M. Cartwright, C. T. Russell, D. N. Baker, and S. G. Kanekal (2006), Acceleration mechanism responsible for the formation of the new radiation belt during the 2003 Halloween solar storm, *Geophys. Res. Lett.*, *33*, L05104, doi:10.1029/2005GL024256.

Stix, T. H. (1992), *Waves in Plasmas*, Am. Inst. of Phys., New York.

Summers, D., R. M. Thorne, and F. Xiao (1998), Relativistic theory of wave particle resonant diffusion with application to electron acceleration in the magnetosphere, *J. Geophys. Res.*, *103*(A9), 20,487–20,500.

Tao, X., A. A. Chan, J. M. Albert, and J. A. Miller (2008), Stochastic modeling of multidimensional diffusion in the radiation belts, *J. Geophys. Res.*, *113*, A07212, doi:10.1029/2007JA012985.

Tao, X., J. M. Albert, and A. A. Chan (2009), Numerical modeling of multidimensional diffusion in the radiation belts using layer methods, *J. Geophys. Res.*, *114*, A02215, doi:10.1029/2008JA013826.

Thorne, R. M., T. P. Armstrong, S. Stone, D. J. Williams, R. W. McEntire, S. J. Bolton, D. A. Gurnett, and M. G. Kivelson (1997), Galileo evidence for rapid interchange transport in the Io torus, *Geophys. Res. Lett.*, *24*(17), 2131–2134.

Thorne, R. M., Y. Y. Shprits, N. P. Meredith, R. B. Horne, W. Li, and L. R. Lyons (2007), Refilling of the slot region between the inner and outer electron radiation belts during geomagnetic storms, *J. Geophys. Res.*, *112*, A06203, doi:10.1029/2006JA012176.

Xiao, F., R. M. Thorne, D. A. Gurnett, and D. J. Williams (2003), Whistler-mode excitation and electron scattering during an interchange event near Io, *Geophys. Res. Lett.*, *30*(14), 1749, doi:10.1029/2003GL017123.

Xiao, F., C. Shen, Y. Wang, H. Zheng, and S. Wang (2008), Energetic electron distributions fitted with a relativistic kappa-type function at geosynchronous orbit, *J. Geophys. Res.*, *113*, A05203, doi:10.1029/2007JA012903.

Xiao, F., Z. Su, H. Zheng, and S. Wang (2009), Modeling of outer radiation belt electrons by multidimensional diffusion process, *J. Geophys. Res.*, *114*, A03201, doi:10.1029/2008JA013580.

Xiao, F., Z. Su, H. Zheng, and S. Wang (2010), Three-dimensional simulations of outer radiation belt electron dynamics including cross-diffusion terms, *J. Geophys. Res.*, *115*, A05216, doi:10.1029/2009JA014541.

D. A. Gurnett and J. D. Menietti, Department of Physics and Astronomy, University of Iowa, Iowa City, IA 52242, USA.

R. B. Horne, British Antarctic Survey, Natural Environment Research Council, Madingley Road, Cambridge CB3 0ET, UK.

B. Ni, Y. Y. Shprits, X. Tao, and R. M. Thorne, Department of Atmospheric and Oceanic Sciences, University of California, Los Angeles, CA 90095, USA. (xtao@atmos.ucla.edu; rmt@atmos.ucla.edu)